

Effect of cobalt addition on shape memory effects in porous TiNi - based alloys obtained by reaction and diffusion sintering

Yasenchuk Yu. F.¹, Artyukhova N. V.¹, Chekalkin T. L.^{1,3*}, Anikeev S. G.¹, Kim Ji-Soon², Kang Ji-Hoon³, Gunther V. E.¹

¹Research Institute of Medical Materials, Tomsk State University, Tomsk, Russia

²School of Materials Science and Engineering, University of Ulsan, Ulsan, South Korea

³Kang & Park Medical Co., O-Song Chungcheongbukdo, South Korea

*Corresponding author. Tel: (+7) 3822-413442; E-mail: tc77@mail2000.ru

Received: 29 June 2015, Revised: 06 April 2016 and Accepted: 28 May 2016

ABSTRACT

Modern medical technologies have developed many new devices that can be implanted into humans to repair, assist or take the place of diseased or defective bones, arteries and even organs. The materials, especially porous ones, used for these devices have evolved steadily over the past twenty years with TiNi-based alloys replacing stainless steels and titanium. The aim of the paper is to present results for examination of porous TiNiMoCo-based alloy intended further to be used in clinical practice. Porous TiNi-based alloys showing shape memory effect were obtained by the methods of reaction and diffusion sintering with cobalt additives. From the results of the analysis of temperature dependences determined by the measurement of electrical resistivity and shape memory effect test, the effect of cobalt addition on the martensitic transformations in sintered body is described. The addition of cobalt during reaction and, especially, diffusion sintering, results in a decrease in the internal stresses in the TiNi phase. The addition of Co more than 1 at. % led to precipitation hardening of the alloy. Cobalt at concentrations studied in the work led to suppression of martensitic phase transformation. Copyright © 2016 VBRI Press.

Keywords: Porous TiNi-based alloy; diffusion sintering; reaction sintering; shape memory effect.

Introduction

A great interest in porous TiNi-based alloys is associated with the fact that they have shape memory effect (SME) and superelastic properties. Due to their biochemical compatibility, it is possible to use them as medical implants for bone tissue replacements [1].

Doping of sintered porous alloys based on TiNi significantly opens up the possibilities of altering their physical and mechanical properties. Doping with cobalt enables the precise adjustment of shape memory parameters. There are few studies on the effect of cobalt on the structure and physico-chemical properties of the alloys obtained by casting [2, 3]. In general, cobalt alloying results in the broadening and shifting of the interval of martensitic transformations towards a decrease in the temperature, as well as in an increase in the amount of residual austenite. However, there are no studies on cobalt doping in sintering of porous TiNi alloys. In general, porous TiNi is sintered by reaction and diffusion methods. In the production of porous TiNi products, these two methods are often used in combination [4-8].

The aim of this work is to study the effect of cobalt addition on the phase structure and shape memory effect in porous TiNi-based alloys produced by diffusion and reaction sintering, respectively.

Experimental

Two types of TiNi specimens were prepared by diffusion and reaction sintering, respectively. For diffusion sintering (DS), prealloyed powder of Ti₄₅Ni₅₅ produced by calcium hydride reduction of the mixture of nickel and titanium oxide was used (Fig. 1). For reaction sintering (RS), electrolytic titanium powder with an average particle size of 60-80 μm and carbonyl nickel powder with an average particle size of 10-15 μm were used (Fig. 2).

Samples with a porosity of 50-60% were prepared by solid-state sintering in a vacuum furnace at 950 °C for 90 min (RS) and at 1270 °C for 5-6 min (DS), respectively. The temperatures of sintering were adjusted empirically with visual assessment of the amount of melting phase on sintered alloys and the level of shrinkage. Shrinkage was controlled with reference to the sample as a whole, as well as the pore size and regularity. Linear shrinkage of the sintered sample was accompanied with shrinkage of pores, which was expressed in the enlargement of pores due to their merger resulting in the formation of cavities. The optimal quality of sintering was defined as the formation of the melt of low-melting phase of Ti₂Ni that is necessary for the formation of strong interparticle necks. In the case of DS, the melt was involved in the formation of the TiNi porous structure by partial dissolution and merger of separate TiNi particles in the porous filling.

Simultaneously, the amount of the melt was kept to a minimum to prevent the processes of shrinkage and enlargement of pores. In the case of RS for powders of titanium and nickel after formation of TiNi at the stage of solid-phase sintering, the melting phase of Ti_2Ni interacted with particles of nickel. As a result of the solid-liquid interaction, an additional phase of TiNi was formed [4, 5].

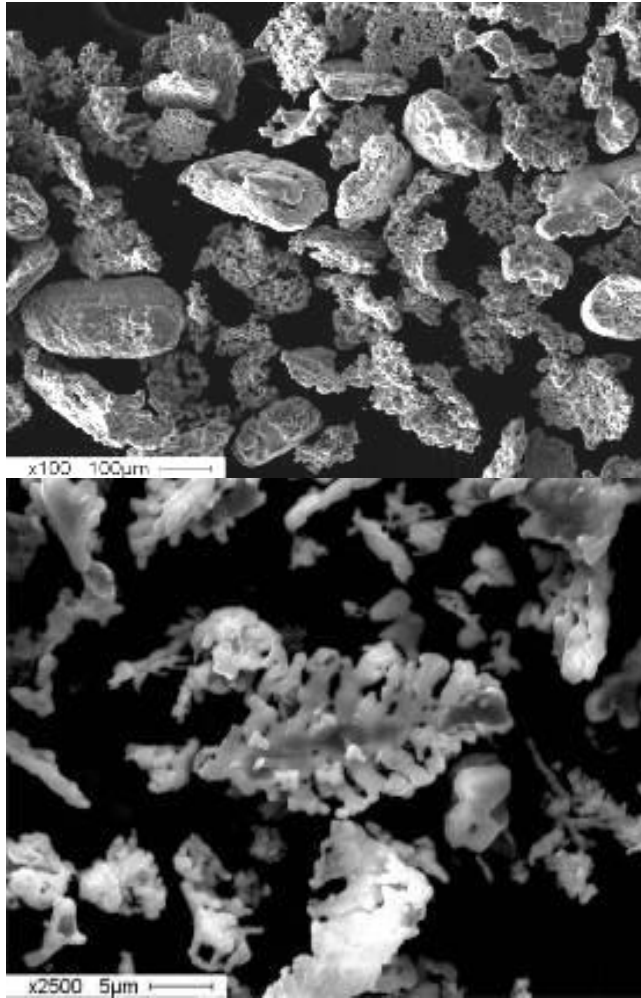
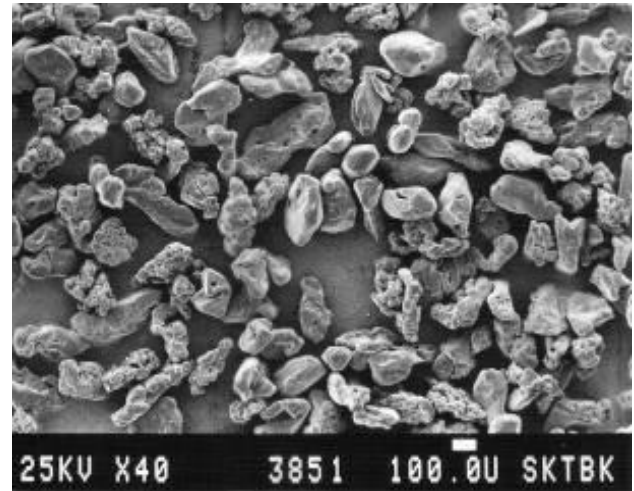


Fig. 1. SEM images of $Ti_{45}Ni_{55}$ powder used for diffusion sintering in the study.

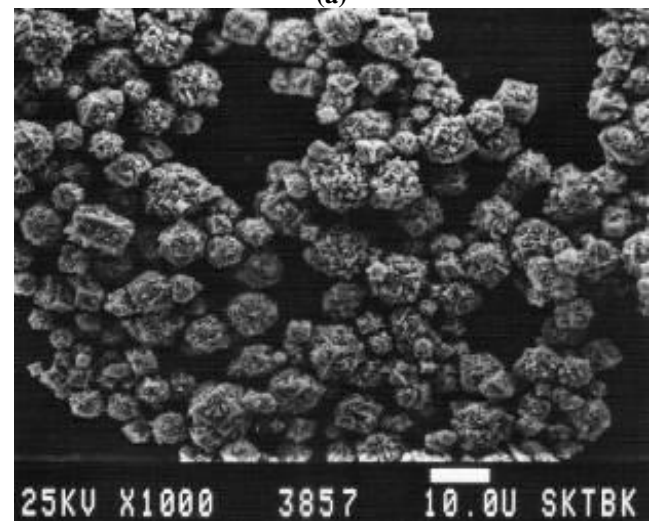
The porous samples as $1 \times 7 \times 35$ mm plates were cut off from the sintered bars by electric discharge process. To evaluate the strain-temperature dependence $\varepsilon(T)$ at SME, the bending 3-point test was carried out within the temperature range -180 to 200 °C under constant load [1]. The heating/cooling rate was 2 °C/min. Samples were maximally deflected to 5.1 mm. All data were computed during the bending and recovering process.

To determine both martensite characteristic points and temperature ranges of martensite transition, the electrical resistivity of the samples was measured by the four-probe method in temperature range from -180 to 100 °C [1, 9]. Ohmic contacts between the probes and samples were made using silver paste. The distance between the middle points along the length of the specimen was 10 mm and the potential difference when the martensitic transition occurs was measured by a digital multimeter. The electrical

resistivity was calculated from the measured potential. A chromel-alumel thermocouple was placed inside the sample body to measure its actual temperature. For tests below room temperature, a liquid nitrogen was applied as the coolant that enabled us to make measurements down to -180 °C, the heating above room temperature was reached by an electrically heated air bath with adjustable power input. During this test the heating/cooling rate was 2 °C/min.



(a)



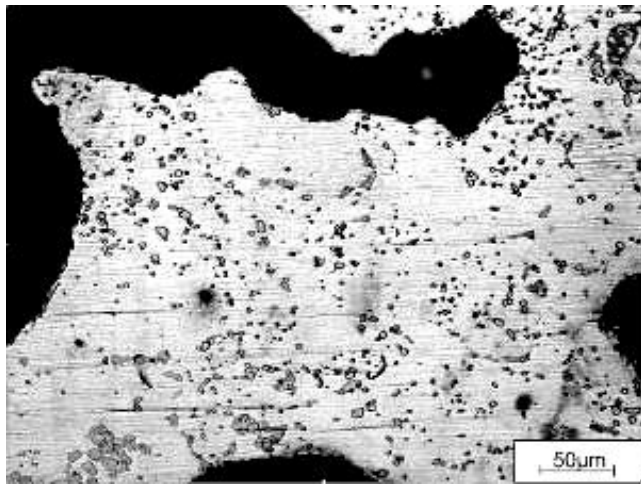
(b)

Fig. 2. SEM images of electrolytic titanium (a) and carbonyl nickel (b) powder used for reaction sintering in the study.

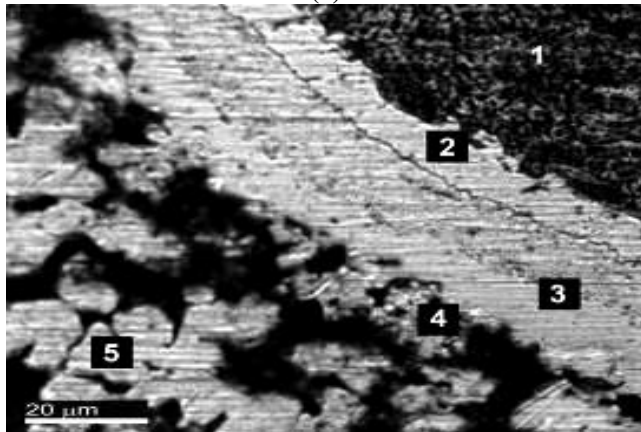
In order to study macro- and microstructure of the samples, thin sections were prepared by means of standard technique. Metallographic examination was conducted using optical microscope Axiovert-40 MAT. Microstructure analysis, phase analysis and topographical studies of pore wall surface were carried out using Philips SEM 515 and Quanta 200 3D. In the work, we used the stereometric image analysis technique for structure evaluation in order to correlate structure evolution with microstructural features such as a grain size and morphology, and also to get information about precipitations and grain boundaries. Details about the applied procedures for data acquisition, data post-processing and analyzing can be found in [10].

Results and discussion

The comparative analysis of the products of both RS and DS enables to make the evaluation of the TiNi phase role in the physical and mechanical properties of the samples. The main distinguishing feature of porous alloys produced by DS is the fact that the TiNi phase occupies about 90% of volume fraction (**Fig. 3**). Porous TiNi produced by solid RS is multiphasic, and the TiNi phase occupy only 20–50% volume percent. In order to increase the proportion of the TiNi phase, RS requires to be brought to the liquid phase stage [4, 5].



(a)



(b)

Fig. 3. SEM images of the alloy structure after DS (a) and RS (b) 1 – Ti, 2 – Ti₂Ni, 3 – TiNi, 4 – TiNi₃, 5 – Ni.

The differences in the temperature dependences of the resistivity $\rho(T)$ in the alloys produced by RS and DS are very large (**Fig. 4**). This is due to the large difference in the amount of the TiNi phase. Besides, in the case of RS, the TiNi phase is formed at the center of reaction cells, and a solid titanium solution in nickel – Ni_γ, which occupies 50–60 vol.% of the sample and which is responsible for its electrical resistivity, forms the periphery [5]. Therefore, the change in the resistivity of the TiNi phase, which is associated with the A→M phase transition and the formation of martensite, weakly manifests itself in the general temperature dependence of the resistivity.

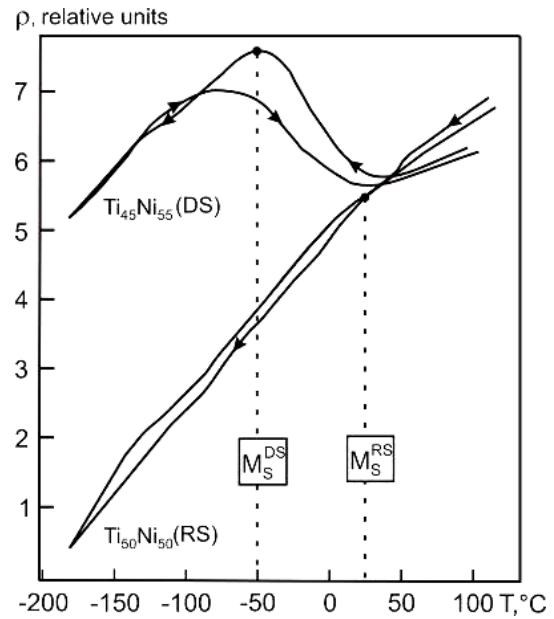


Fig. 4. Comparative resistivity-temperature test of DS and RS sample.

The temperature dependence of the electrical resistivity of porous TiNi produced by DS (**Fig. 5**) has a sharp maximum in the area of martensite transformation, martensite-austenite (A→M). The slightest addition of cobalt leads to a sharp decrease in the extreme value of the electrical resistivity. Simultaneously with a decrease, the maximum is expanded. Such a behavior of the dependence is in good agreement with the results of X-ray diffraction studies of porous TiNi [11]. The comparison of the results leads to the conclusion that the reduction and expansion of the maximum of the dependence of electrical resistivity at the area of A→M transition in the case of addition of cobalt at 0.5 to 2.0 at.% corresponds to an increase in residual austenite, a decrease in the completeness of direct A→M transformation, and its smooth deceleration.

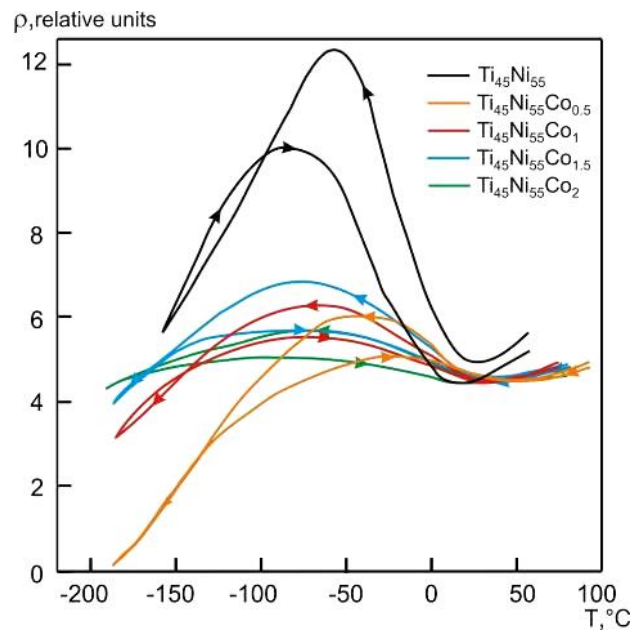


Fig. 5. Comparative resistivity-temperature dependencies of DS samples with cobalt additives.

The expansion of the temperature interval of martensitic transformation towards low temperatures associated with the quantitative growth of residual austenite is characteristic of isothermal martensite formation. Sometimes, such an effect is called blurring of the martensitic transformation [13].

The effect of cobalt additives on the deformation properties of both RS and DS samples is manifested in a similar way. However, for the DS sample, the dependence is more pronounced (Fig. 6). In the dependence of the multiple shape memory effect, three components of deformation are distinguished [1]: initial irreversible $\epsilon_{\text{irrev}}^{\text{cool}}$, maximum accumulated $\epsilon_{\text{rev}}^{\text{cool}}$, and residual $\epsilon_{\text{res}}^{\text{heat}}$ as a result of the parent-martensite-parent phase transition cycle ($A \leftrightarrow M$) under load. These components are strongly influenced by the concentration of cobalt added. This influence can be divided into four stages.

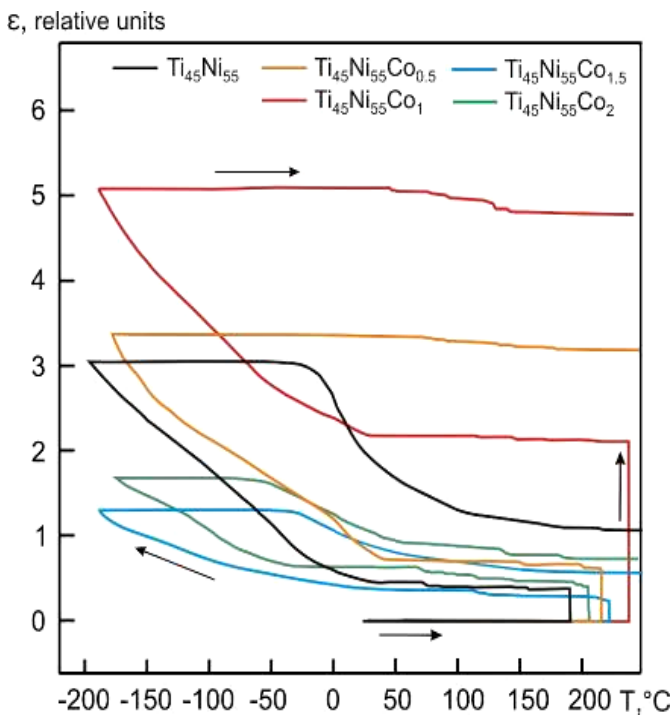


Fig. 6. SME comparative strain-temperature test of DS samples with cobalt additives.

In the first stage, the addition of 0.5 at.% of Co results in a sharp increase in the residual strain because of the phase transformation cycle, $A \leftrightarrow M$. In the second stage, with an increase in the cobalt concentration of 0.5 to 1 at.%, a gradual increase in the ductility of the austenitic phase and a slight increase in the reversal strain in the $M \rightarrow A$ transition are observed. The effect of additives on the maximum accumulated strain during $A \rightarrow M$ transition is nearly undetectable at these concentrations. In the third stage, at the cobalt concentration of 1.0 to 1.5 at.%, a sharp decrease in all the components of deformation is observed due to the increased role of the precipitation hardening of the austenitic phase in the sintered alloy. In the fourth stage, an increase in the cobalt concentration of higher than 1.5 at.% has no significant effect on the parameters of the shape memory, while at the same time, significantly

increases both the amount of formed melt and the sinterability of the TiNi powder.

The sample prepared by DS with no Co addition has similar properties as that prepared by RS, *i.e.*, it exhibited high reversible martensite deformation. This indicates a high level of internal stresses in the TiNi phase that is typical for RS. We assume that DS is accompanied with elements of RS, since we observed that the concentration of components of the TiNi powder particles varies in terms of the ratio of $Ti_{1-x}Ni_x$ (where $x=27.13-72.18$ at.%) due to the technological characteristics of the technology to produce the powder by the method of calcium hydride reduction [12]. This assumption is confirmed by the observed areas of the TiNi phase in the diffusion interparticle necks in samples produced by DS (Fig. 7).

At cobalt concentrations of 1.0 to 2.0 at.%, the level of internal stresses in TiNi also increases, but rather due to the diffusion hardening of austenite. This leads to regrowth of the reversal martensite deformation, comparable with that of the maximum accumulated one.

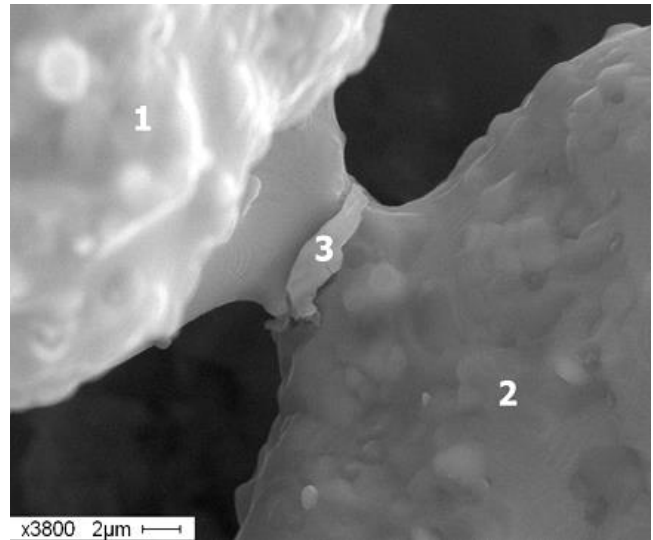


Fig. 7. SEM of $Ti_{1-x}Ni_x$ phases in the diffusion interparticle neck-like area: 1 – 48.87 to 54.04, 2 – 41.02 to 47.30, 3 – 45.43 to 51.70 at.% of Ni.

For RS of porous TiNi with the addition of cobalt, deformation properties of the $Ti_{50}Co_{50}$ alloy are almost similar to properties of the $Ti_{50}Ni_{50}$ binary alloy (Fig. 8). Addition of 1 at.% of Co to 49 at.% of Ni during RS leads to significant differences in the values of $\epsilon_{\text{irrev}}^{\text{cool}}$, $\epsilon_{\text{res}}^{\text{heat}}$,

$$\epsilon_{\text{rev}}^{\text{cool}}.$$

The distinctive properties of samples prepared by RS are exemplified by the fact that they maintain reversible deformation almost constant, regardless of the amount of cobalt added, under the external stress. Since reversible strain is associated with a change in the quantity of martensite, it may be concluded that the newly formed TiNi phase has a high level of intrinsic stresses in the diffusion powder Ti-Ni pair. Therefore, the addition of stresses from the external load counteracting the reduction of the shape is not essential. The effect of cobalt on the level of intrinsic stresses is also of less significance.

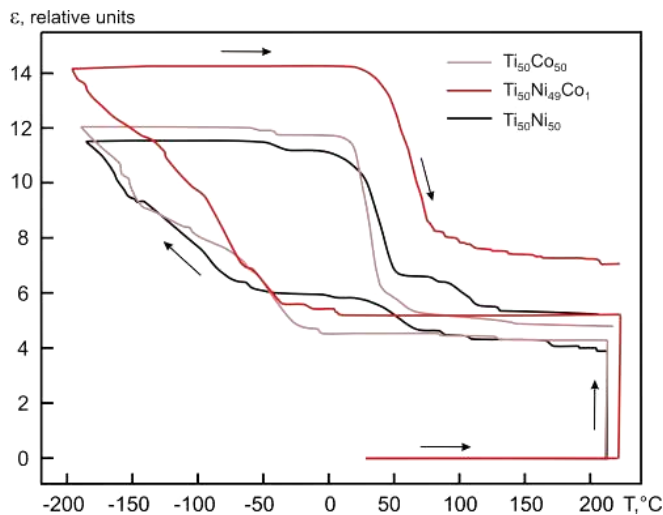


Fig. 8. SME comparative strain-temperature test of RS samples with cobalt additives.

Conclusion

Based on the above results, it can be concluded that the addition of cobalt always interferes martensitic phase transformation.

Due to the addition of 0.5–1 at.% of Co during diffusion sintering, the level of intrinsic stresses in the austenite is significantly decreased. As a result, the external load in the case of multiple shape memory effects hinders the completion of the reverse martensitic transition. In the case of additions of more than 1 at.% of Co, a further reduction of stresses makes it impossible to complete the direct martensitic transformation under the influence of the temperature factor alone. The addition of 1–2 at.% of Co, due to precipitation hardening, leads to an increase in stresses in the austenite that leads to the occurrence of reverse martensitic transformation under load.

However, the influence of internal stresses in the austenite is not the same. Inherent stresses accelerate the martensitic transformation, whereas stresses induced by precipitation hardening restrain it.

Acknowledgements

This study (research grant No 8.1.42.2015) was supported by the Tomsk State University Academic D.I. Mendeleev Fund Program in 2015. The authors gratefully acknowledge the support for this research provided by the Tomsk State University Competitiveness Improvement Program. The support is greatly appreciated.

Reference

1. Gunther, V.E., Hodorenko, V.N., Chekalkin TL *et al.*, Medical materials and shape memory implants: In 14 vol. / *Shape memory medical materials*. Tomsk: MIC; 2011, 1.
ISBN: 978-5-9858-9044-0
2. Bhagyaraj, J.; Ramaiah, K.V.; Saikrishna, C.N.; Bhaumik, S.K. *J Alloy Compd.* 2013, 581, 344.
DOI: 10.1016/j.jallcom.2013.07.046
3. El-Bagoury, N. *Mater Sci Tech.* 2014, 30, 1795.
DOI: 10.1179/1743284713Y.0000000478
4. Yasenchuk, Yu.F.; Artyukhova, N.V.; Novikov, V.A.; Gyunter, V.E. *Tech Phys Lett.* 2014, 40, 697.
DOI: 10.1134/S1063785014080276
5. Artukhova, N.V.; Yasenchuk, Yu.F.; Kim, J.S.; Gunther, V.E. *Russ Phys J.* 2015, 57, 1313.

DOI: 10.1007/s11182-015-0383-2

6. Anikeev, S.G.; Khodorenko, V.N.; Kokorev, O.V.; Chekalkin, T.L. *Adv Mater Res.* 2015, 1085, 430.
DOI: 10.4028/www.scientific.net/AMR.1085.430
7. Gunther, V.E.; Chekalkin, T.L.; Kim, J.S.; Hodorenko, V.N. *Adv Mater Lett.* 2015, 6, 8.
DOI: 10.5185/amlett.2015.5597
8. Bansiddhi, A.; Dunand, D.C. *J Mater Eng Perform.* 2011, 20, 511.
DOI: 10.1007/s11665-010-9827-6
9. Al-Aql, A.A.; Dughaish, Z.H.; Baig M.R. *Mater Lett.* 1993, 17, 103
DOI: 10.1016/0167-577X(93)90066-7
10. ASTM Standard E112-13 / *West Conshohocken: ASTM International*, 2014.
DOI: 10.1520/E0112
11. Gyunter, V.E.; Khodorenko, V.N.; Monogenov, A.N.; Yasenchuk, Yu.F. *Tech Phys Lett.* 2000, 26, 320.
DOI: 10.1134/1.1262830
12. Malygin, G.A. *Phys Uspek.* 2001, 44, 173.
DOI: 10.1070/PU2001v044n02ABEH000760
13. Yi, H.C.; Moore, J.J. *J Mater Sci.* 1989, 24, 3449.
DOI: 10.1007/BF02385723

A Monthly Journal

Publish your article in this journal

Advanced Materials Letters is an official international journal of International Association of Advanced Materials (IAAM, www.iaamonline.org) published monthly by VBRI Press AB from Sweden. The journal is intended to provide high-quality peer-review articles in the fascinating field of materials science and technology particularly in the area of structure, synthesis and processing, characterisation, advanced-state properties and applications of materials. All published articles are indexed in various databases and are available download for free. The manuscript management system is completely electronic and has fast and fair peer-review process. The journal includes review article, research article, notes, letter to editor and short communications.

Copyright © 2016 VBRI Press AB, Sweden

www.vbripress.com/aml